

Synthesis and Structure Determination of Rh–diene Complexes with the Hydridotris(3,5-diisopropylpyrazolyl)borate Ligand, $\text{Tp}^{\text{iPr}}\text{Rh}(\text{diene})$ (diene = cod, nbd): Dependence of the $\nu(\text{B–H})$ Values on the Hapticity of the Tp^{iPr} Ligand (κ^2 vs κ^3)¹

Munetaka Akita,* Keisuke Ohta, Yoshiaki Takahashi, Shiro Hikichi, and Yoshihiko Moro-oka*

Research Laboratory of Resources Utilization, Tokyo Institute of Technology, 4259 Nagatsuta, Midori-ku, Yokohama 226, Japan

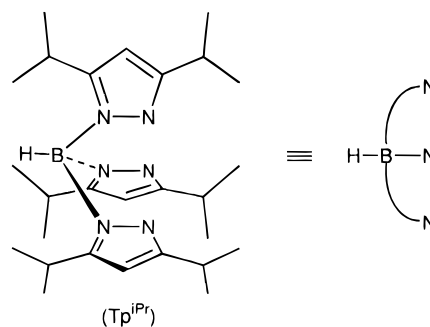
Received April 24, 1997[Ⓢ]

Rhodium–diene complexes with the Tp^{iPr} ligand, $\text{Tp}^{\text{iPr}}\text{Rh}(\text{diene})$ (Tp^{iPr} = hydridotris(3,5-diisopropylpyrazolyl)borate; diene = 1,5-cyclooctadiene (cod) (**1**), norbornadiene (nbd) (**2**)), are prepared by treatment of $[\text{Rh}(\mu\text{-Cl})(\text{diene})]_2$ with KTp^{iPr} or TlTp^{iPr} . The structure of **1**, characterized by X-ray crystallography, contains the κ^2 -coordinated Tp^{iPr} ligand, and its central Rh atom adopts a square-planar geometry, whereas the unit cell of **2** contains two independent molecules: a square-planar structure with a κ^2 -coordinated Tp^{iPr} ligand similar to **1** and a trigonal-bipyramidal one with a κ^3 -coordinated Tp^{iPr} ligand. Although ¹H and ¹³C NMR spectroscopy does not provide any information concerning the coordination geometry due to the interconversion between the square-planar and trigonal-bipyramidal structures, which occurs at a rate much faster than the NMR time scale, IR analysis reveals that the bands observed around 2470 and 2540 cm^{-1} are assigned to the B–H stretching vibrations of the square-planar and trigonal-bipyramidal structures, respectively. Thus, the $\nu(\text{B–H})$ value can be used as an indicator of the hapticity of a Tp^{iPr} ligand (κ^2 ($\sim 2470 \text{ cm}^{-1}$) vs κ^3 ($> 2530 \text{ cm}^{-1}$)) as compared with related $\text{Tp}^{\text{iPr}}\text{ML}_n$ -type complexes.

Introduction

Hydridotris(pyrazolyl)borate (Tp) has been recognized as a versatile ligand in the field of transition-metal chemistry.² It is a mononegative 6e donor similar to the cyclopentadienyl ligand (Cp) which has been widely used as an auxiliary ligand for organometallic compounds, and a number of analogous TpML_n - and CpML_n -type complexes and their ring-substituted derivatives ($\text{Tp}^{\text{R}}\text{ML}_n$ and $(\eta^5\text{-C}_5\text{R}_5)\text{ML}_n$) have been prepared so far. The Tp^{R} ligand is able to tune the electronic and steric environment of the central metal atoms by introducing various substituents to the pyrazolyl ring. In addition to this feature, a coordination environment created by the Tp^{R} ligand can mimic an environment created by a set of three imidazole rings of histidine residues which is frequently found in the metal coordination site of metalloproteins. In our laboratory, the structure and functions of the metal centers in metalloproteins have been studied from the bioinorganic viewpoint by using Tp^{R} ligands, in particular, hydridotris(3,5-diisopropylpyrazolyl)borate (Tp^{iPr} ; Chart 1).³ As a result, studies on coordination chemistry of the first-

Chart 1



row transition-metal complexes (Mn, Fe, Co, Ni, and Cu) have led to successful analysis of many aspects of oxygen metabolism, as typically exemplified by the prediction of the $(\mu\text{-}\eta^2\text{:}\eta^2\text{-O}_2)\text{Cu}_2$ structure in hemocyanin.⁴ Recently we have extended our synthetic study to complexes of the second- and third-row transition metals. Though they are seldom found in nature, comparison of the structure and chemical properties of the first-row metal complexes with those of their heavier congeners would provide us with insight into the role of the central metal atoms in various catalytic and biological functions, and they might possibly display unique reactivity applicable to organic transformations.

Herein we disclose details of the synthesis and structure of $\text{Tp}^{\text{iPr}}\text{Rh}(\text{diene})$ complexes (diene = 1,5-

[Ⓢ] Abstract published in *Advance ACS Abstracts*, August 15, 1997.

(1) Abbreviations used in this paper: Tp, hydridotris(pyrazolyl)borate; Tp^{iPr} , hydridotris(3,5-diisopropylpyrazolyl)borate; Tp^{R} , substituted Tp derivatives; pz, pyrazolyl group; cod, 1,5-cyclooctadiene; nbd, norbornadiene; *spl*, square planar; *tbp*, trigonalbipyramidal.

(2) (a) Trofimenko, S. *Chem. Rev.* **1993**, *93*, 943. (b) Kitajima, N.; Tolman, W. B. *Prog. Inorg. Chem.* **1995**, *43*, 419.

(3) (a) Kitajima, N.; Moro-oka, Y. *Chem. Rev.* **1994**, *94*, 737. (b) See also the special issue of *Chem. Rev.* on "Bioinorganic Enzymology": *Chem. Rev.* **1996**, *96*, 2237–3042.

(4) Kitajima, N.; Fujisawa, K.; Fujimoto, C.; Moro-oka, Y.; Hashimoto, S.; Kitagawa, T.; Toriumi, K.; Tatsumi, K.; Nakamura, A. J. *Am. Chem. Soc.* **1992**, *114*, 1277.

Table 1. B–H Stretching Vibrations of **1** and **2**^a

complex	diene	hapticity of Tp ^{iPr} ligand ^b	$\nu(\text{B-H})^c$	KBr	MeCN	CHCl ₃	CH ₂ Cl ₂	hexane
1	cod	κ^2	I	2475	2479	2482	2479	2479
			II	n.d. ^d	n.d.	n.d.	n.d.	n.d.
			I/II ^e	100/0	100/0	100/0	100/0	100/0
2	nbd	$\kappa^2 + \kappa^3$	I	2472	2479	2482	2481	2476
			II	2539	2548	2543	2545	2539
			I/II ^e	50/50	60/40	50/50	55/45	55/45

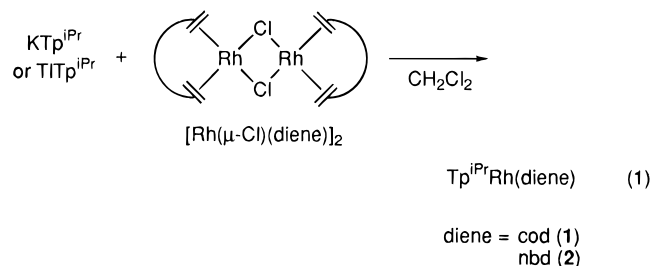
^a $\nu(\text{B-H})$ in cm^{-1} . ^b Hapticity of the Tp^{iPr} ligand revealed by X-ray crystallography. ^c IR absorptions observed around 2470 and 2550 cm^{-1} are denoted as **I** and **II**, respectively. ^d Not detected. ^e Intensity ratio of the two absorptions, **I** and **II**.

cyclooctadiene (cod) (**1**), norbornadiene (nbd) (**2**)). The Tp^RRhL₂-type rhodium complexes (L = diene, olefin, CO, PR'₃, NCR'; R = substituents of the pyrazolyl rings)^{5–7} have been studied extensively, and the following structural aspects arising from the hapticity change of the Tp^R ligand are revealed mainly by using NMR techniques and X-ray crystallography: (1) Tp^RRhL₂ adopts either the square-planar (*spl*) geometry (two isomers are possible, as will be discussed later) or the trigonal-bipyramidal (*tbp*) geometry, where the Tp^R ligand works as a bidentate (κ^2) and tridentate ligand (κ^3), respectively, and the geometry depends on the other ligands (L) and the pyrazolyl substituents (R); (2) the three structures are usually interconverted with each other, and the three pyrazolyl rings often become equivalent at a higher temperature as observed by NMR. However, let us point out that, although intense IR absorptions such as CO stretching vibrations have been discussed as a probe for the coordination geometry,⁶ little attention has been paid to the $\nu(\text{B-H})$ vibration which is generally observed for Tp^RML_n-type complexes. Correlation between the B–H stretching vibration and the hapticity of the Tp^R ligand will also be discussed in this paper.

Results

Synthesis and Spectroscopic Characterization of Tp^{iPr}Rh(diene). The Rh–diene complexes Tp^{iPr}Rh(diene) (diene = cod (**1**), nbd (**2**)) were obtained by treatment of [RhCl(diene)]₂ with KTp^{iPr} in CH₂Cl₂

following the procedure reported for the Tp^R derivatives (eq 1).^{5a,d,e,f} The thallium reagent, TITp^{iPr}, could be used in place of the potassium salt.



The composition of the products, Tp^{iPr}Rh(diene), was readily confirmed by ¹H and ¹³C NMR spectra, and their coordinated olefinic carbon atoms were located at δ_{C} 79.4 (**1**) and 42.8 (**2**). However, because all three pyrazolyl rings in the Tp^{iPr} ligands of **1** and **2** were equivalent even at -80°C (at 270 MHz (¹H) and 67 MHz (¹³C)), no information concerning the coordination geometry around the Rh center could be obtained by the NMR study.

It is noteworthy that IR spectra of **1** recorded in the solid state and in solution contained only one $\nu(\text{B-H})$ vibration at $\sim 2470 \text{ cm}^{-1}$, whereas those of **2** contained two $\nu(\text{B-H})$ vibrations at ~ 2470 (**I**) and $\sim 2550 \text{ cm}^{-1}$ (**II**) (Figure 1 and Table 1). No significant solvent effect on the absorption maxima and the intensity ratio (**I/II**) was observed.

X-ray Crystallography of Tp^{iPr}(diene). In order to compare the solid-state structures of **1** and **2** with those of related TpRhL₂-type complexes, their molecular structures have been determined by X-ray crystallography. Overviews and selected structural parameters are shown in Figures 2–4 and Table 2.

The structure of the cod complex **1** can be described as an *spl* Rh complex where the Tp^{iPr} ligand is coordinated to the Rh center through two of the three pyrazolyl rings. The sum of the angles around Rh formed by the coordinated pyrazolyl nitrogen atoms (N11 and N21) and the midpoints of the olefinic carbon atoms (M1 (C1–C2) and M2 (C5–C6)) (364.1°) clearly indicates the planarity of the N₂Rh(diene) moiety, which has local mirror symmetry as judged by the almost equal Rh1–N (N11 and N21) and Rh1–olefinic carbon atom (C1, C2, C5, and C6) distances. The noncoordinated pyrazolyl ring is cofacial with respect to the N₂-Rh(diene) plane. However, no π -interaction with the Rh center is present, because the distance from the noncoordinated pyrazolyl nitrogen atom (N31) to Rh1 ($3.719(3) \text{ \AA}$) is out of the range of the bonding interaction (the sum of van der Waals radii: 3.15 \AA). Other structural parameters are in the range of accepted values.

(5) Diene complexes: (a) Cocivera, M.; Desmond, T. J.; Ferguson, G.; Kaitner, B.; Lalor, F. J.; O'Sullivan, D. J. *Organometallics* **1982**, *1*, 1125. (b) Cocivera, M.; Ferguson, G.; Kaitner, B.; Lalor, F. J.; O'Sullivan, D. J.; Parvez, M.; Ruhl, B. *Organometallics* **1982**, *1*, 1132. (c) Cocivera, M.; Ferguson, G.; Lalor, F. J.; Szczecinski, P. *Organometallics* **1982**, *1*, 1139. (d) Bucher, U. E.; Currao, A.; Nesper, R.; Rügger, H.; Venanzi, L. M.; Younger, E. *Inorg. Chem.* **1995**, *34*, 66. (e) Bucher, U. E.; Fässler, T. F.; Hunziker, M.; Nesper, R.; Rügger, H.; Venanzi, L. M. *Gazz. Chim. Ital.* **1995**, *125*, 181. (f) Sanz, D.; Santa Maria, M. D.; Claramunt, R. M.; Cano, M.; Heras, J. V.; Campo, J. A.; Ruiz, F. A.; Pinilla, E.; Monge, A. *J. Organomet. Chem.* **1996**, *526*, 341.

(6) CO and isonitrile complexes: (a) Trofimenko, S. *Inorg. Chem.* **1971**, *10*, 1372. (b) May, S.; Reissalu, P.; Powell, J. *Inorg. Chem.* **1980**, *19*, 1582. (c) Ghosh, C. K.; Graham, W. A. G. *J. Am. Chem. Soc.* **1987**, *109*, 4726. (d) Ghosh, C. K.; Graham, W. A. G. *J. Am. Chem. Soc.* **1989**, *111*, 375. (e) Jones, W. D.; Hessel, E. T. *Inorg. Chem.* **1991**, *30*, 778. (f) Hessel, E. T.; Jones, W. D. *Organometallics* **1992**, *11*, 1496. (g) Jones, W. D.; Hessel, E. T. *J. Am. Chem. Soc.* **1992**, *114*, 6087. (h) Jones, W. D.; Hessel, E. T. *J. Am. Chem. Soc.* **1993**, *115*, 554. (i) Rheingold, A. L.; Ostrander, R. L.; Haggerty, B. S.; Trofimenko, S. *Inorg. Chem.* **1993**, *33*, 3666. (j) Keyes, M. C.; Young, V. G., Jr.; Tolman, W. B. *Organometallics* **1996**, *15*, 4133. (k) Chauby, V.; Le Berre, S.; Daran, J.-C.; Commenges, G. *Inorg. Chem.* **1996**, *35*, 6345. (l) Connelly, N. G.; Emslie, D. J. H.; Metz, B.; Orpen, A. G.; Quayle, M. J. *J. Chem. Soc., Chem. Commun.* **1996**, 2289. (m) Purwoko, A. A.; Lees, A. J. *Inorg. Chem.* **1996**, *35*, 675. (n) Dhosh, C. K.; Rodgers, D. P. S.; Graham, W. A. G. *J. Chem. Soc., Chem. Commun.* **1988**, 1511.

(7) Olefin complexes: (a) Trofimenko, S. *J. Am. Chem. Soc.* **1969**, *91*, 588. (b) Oldham, W. J.; Heinekey, D. M. *Organometallics* **1997**, *16*, 467. (c) Pérez, P. J.; Poveda, M. L.; Carmona, E. *Angew. Chem., Int. Ed. Engl.* **1995**, *34*, 66.

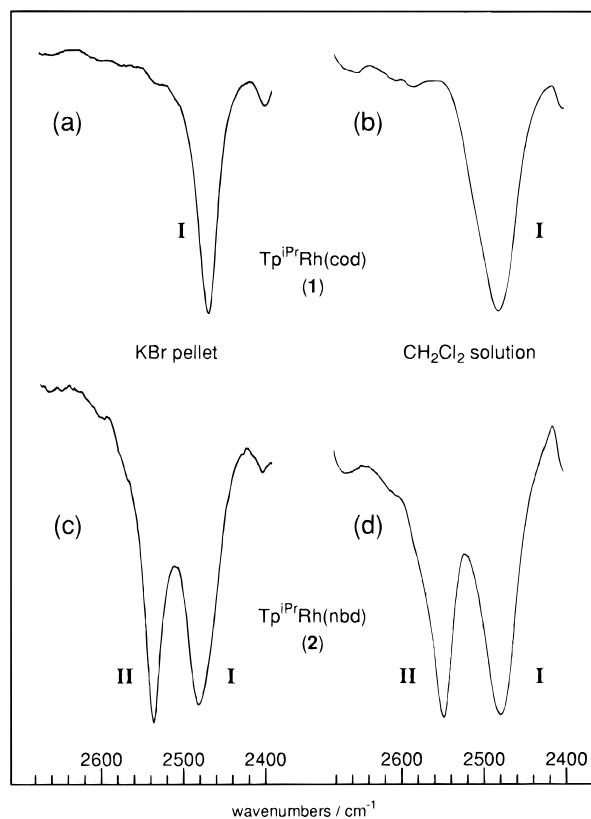


Figure 1. $\nu(\text{B-H})$ region of the IR spectra of **1** and **2**: (a) **1** in KBr; (b) **1** in CH_2Cl_2 ; (c) **2** in KBr; (d) **2** in CH_2Cl_2 .

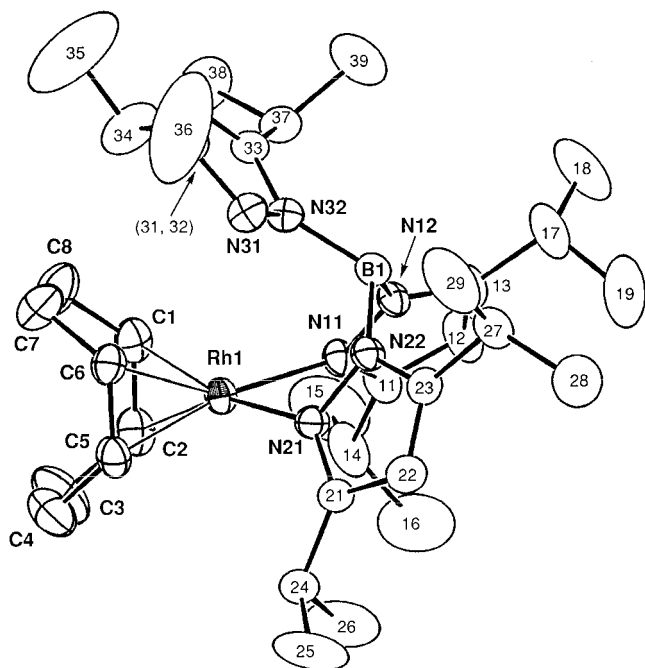


Figure 2. Molecular structure of **1** drawn at the 30% probability level. The labels without atom names are for the Tp^{iPr} carbon atoms.

On the other hand, the unit cell of the nbd complex **2** contains two crystallographically independent molecules with different coordination geometries. One is an *spl* structure (molecule 1), and the other is a *tbp* structure (molecule 2).

The coordination geometry of molecule 1 is described as an *spl* one, and the core structure is essentially the same as that of the cod complex **1** mentioned above,

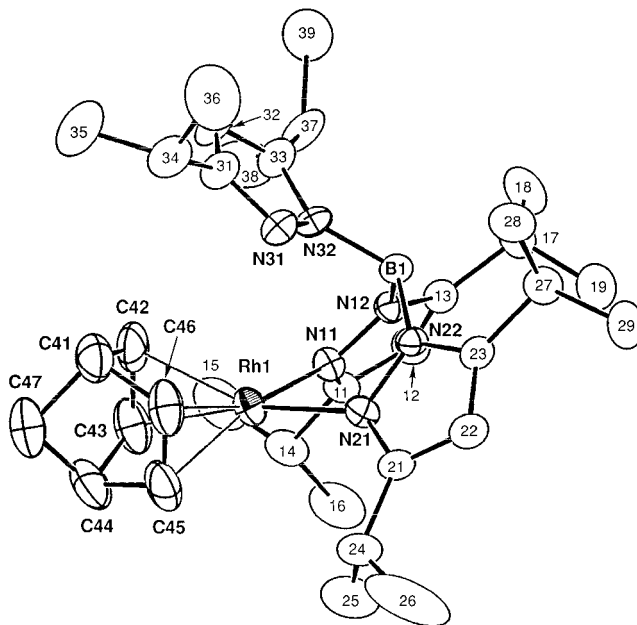


Figure 3. Molecular structure of **2** (molecule 1) drawn at the 30% probability level. The labels without atom names are for the Tp^{iPr} carbon atoms.

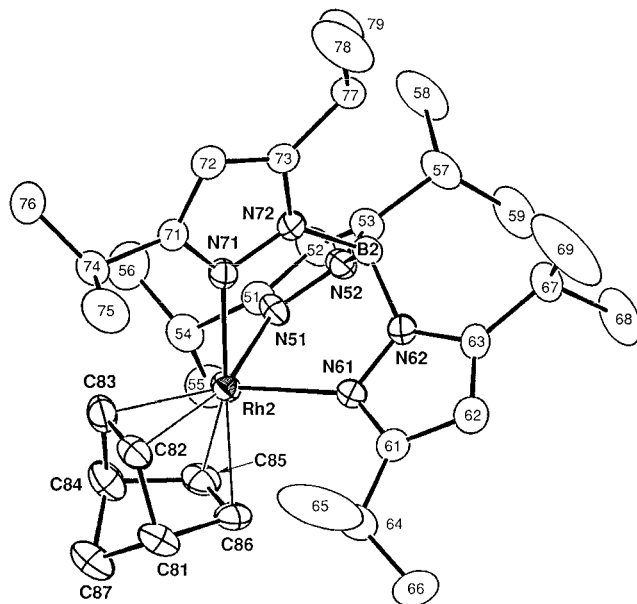


Figure 4. Molecular structure of **2** (molecule 2) drawn at the 30% probability level. The labels without atom names are for the Tp^{iPr} carbon atoms.

though the angles associated with the nbd ligand (M3-Rh1-M4 , 70.3°) are smaller than those of **1** (M1-Rh1-M2 , 86.9°) because of the smaller bite angle formed by the olefinic parts in nbd.

In contrast to molecule 2, coordination of all the three pyrazolyl rings to the Rh center in molecule 2 leads to a *tbp* structure with the axis passing through N71-Rh2-M6 (M6 , midpoint of C85-C86), as judged by (1) the Rh2-N71 distance ($2.146(4) \text{ \AA}$) being shorter than the other two Rh2-N61 ($2.260(4) \text{ \AA}$) and Rh2-N71 distances ($2.273(4) \text{ \AA}$) and (2) the linear N71-Rh2-M6 linkage (174.3°). In accord with this description, the N51-Rh2-N61 angle (90.4°) in the equatorial plane is larger than the other two N-Rh2-N angles ($\sim 82^\circ$) so as to be closer to the ideal ligand angle (120°) so the sum of the equatorial ligand angles (359.9°) indicates

Table 2. Selected Structural Parameters for **1** and **2**^a

complex 1 square planar		complex 2			
		square planar (molecule 1)		trigonal bipyramidal (molecule 2)	
Interatomic Distances (Å)					
Rh1–N11	2.133(3)	Rh1–N11	2.134(4)	Rh2–N51	2.260(4)
Rh1–N21	2.099(3)	Rh1–N21	2.119(4)	Rh2–N61	2.273(4)
Rh1...N31	3.719(3)	Rh1...N31	3.392(4)	Rh2–N71	2.146(4)
Rh1–C1	2.142(4)	Rh1–C42	2.105(6)	Rh2–C82	2.074(5)
Rh1–C2	2.131(4)	Rh1–C43	2.117(5)	Rh2–C83	2.069(5)
Rh1–C5	2.135(4)	Rh1–C45	2.119(6)	Rh2–C85	2.137(5)
Rh1–C6	2.126(4)	Rh1–C46	2.096(5)	Rh2–C86	2.149(4)
Rh1–M1	2.024	Rh1–M3	1.993	Rh2–M5	1.941
Rh1–M2	2.016	Rh1–M4	1.993	Rh2–M6	2.032
C1–C2	1.367(6)	C42–C43	1.389(8)	C82–C83	1.448(6)
C5–C6	1.378(6)	C45–C46	1.367(8)	C85–C86	1.364(6)
Bond Angles (deg)					
C1–Rh1–C2	37.3(2)	C42–Rh1–C43	38.4(2)	C82–Rh2–C83	40.9(2)
C1–Rh1–C5	94.2(2)	C42–Rh1–C45	78.2(2)	C82–Rh2–C85	79.5(2)
C1–Rh1–C6	81.0(2)	C42–Rh1–C46	66.6(3)	C82–Rh2–C86	66.7(2)
C1–Rh1–N11	93.6(1)	C42–Rh1–N11	103.5(2)	C82–Rh2–N51	154.2(2)
C1–Rh1–N21	167.7(2)	C42–Rh1–N21	148.7(2)	C82–Rh2–N61	154.2(2)
C2–Rh1–C5	81.5(2)	C43–Rh1–C45	65.2(3)	C83–Rh2–C85	66.0(2)
C2–Rh1–C6	92.1(2)	C43–Rh1–C46	79.3(2)	C83–Rh2–C86	79.9(2)
C2–Rh1–N11	100.8(2)	C43–Rh1–N11	102.3(2)	C83–Rh2–N51	113.3(2)
C2–Rh1–N21	154.9(2)	C43–Rh1–N21	168.6(2)	C83–Rh2–N61	156.2(2)
C5–Rh1–C6	37.7(2)	C45–Rh1–C46	37.8(2)	C85–Rh2–C86	37.1(2)
C5–Rh1–N11	169.6(2)	C45–Rh1–N11	158.1(2)	C85–Rh2–N51	88.3(2)
C5–Rh1–N21	91.1(1)	C45–Rh1–N21	105.0(2)	C85–Rh2–N61	114.9(2)
N11–Rh1–N21	82.5(1)	N11–Rh1–N21	85.0(1)	N51–Rh2–N61	90.4(1)
N11–Rh1–M1	97.6	N11–Rh1–M3	103.6	N51–Rh2–M5	133.7
N11–Rh1–M2	169.2	N11–Rh1–M4	173.6	N51–Rh2–M6	102.0
N21–Rh1–M1	173.5	N21–Rh1–M4	166.3	N61–Rh2–M5	135.8
N21–Rh1–M2	97.1	N21–Rh1–M4	101.3	N61–Rh1–M6	101.9
M1–Rh1–M2	86.9	M3–Rh1–M4	70.3	M5–Rh2–M6	71.0
				N71–Rh2–C82	102.2(2)
				N71–Rh2–C83	102.8(2)
				N71–Rh2–C85	161.2(2)
				N71–Rh2–C86	160.0(2)
				N71–Rh2–N51	82.5(1)
				N71–Rh2–N61	81.5(1)
				N71–Rh2–M5	103.3
				N71–Rh2–M6	174.3

^a M1, M2, M3, M4, M5, and M6 refer to the midpoints of C1–C2 and C5–C6 (**1**) and C42–C43, C45–C46, C82–C83, and C85–C86 (**2**), respectively.

the planarity of the Rh2–N51–N61–M5 moiety (M5, midpoint of C82–C83), but the equatorial plane is not perpendicular to the N71–Rh2–M6 axis because of the small bite angle of the nbd ligand (71.0°).

Discussion

Structure of TpⁱPrRh(diene) Complexes. To our knowledge, nine [poly(pyrazolyl)borato]Rh(diene) complexes have been characterized by X-ray crystallography: [κ^2 -B(pz)₄]Rh(cod) (**3**),^{5a-c} [κ^2 -B(pz)₄]Rh(nbd) (**4**),^{5a-c} [κ^3 -B(pz)₄]Rh(duroquinone) (**5**),^{5a-c} [κ^3 -HB(3-Me-pz)₃]Rh(nbd) (**6**),^{5d} [κ^3 -MeB(3-Me-pz)₃]Rh(nbd) (**7**),^{5e} [κ^2 -HB(3-Ph-pz)₃]Rh(nbd) (**8**),^{5f} [κ^2 -HB(3-Ph-pz)₃]Rh(cod) (**9**),^{5f} and our complexes [κ^2 -HB(3,5-Prⁱ-pz)₃]Rh(cod) (**1**) and [κ^2 - and κ^3 -HB(3,5-Prⁱ-pz)₃]Rh(nbd) (**2**). Although it is well-known that 16e d⁸ Rh complexes favor the *spl* geometry, the presence of the free pyrazolyl ring proximal to the axial, coordinatively unsaturated site may lead to the *tbp* structure. The hapticity of the poly(pyrazolyl)borato ligand (κ^2 vs κ^3) may depend on (1) the structure and properties of the diene and (2) the substitution pattern of the pyrazolyl rings, but no clear-cut explanation has been proposed so far. As for point 1, it may be concluded that complexes with a diene having a larger bite angle such as cod favor a κ^2 structure, judging from the fact that only a κ^2 structure has been found for cod

complexes.^{8–18} However, TpRh(cod) adopts a *tbp* structure, as judged by its NMR data.^{5d} Therefore, the above conclusion is not always correct. In the case of the nbd complexes (**4**, **6**, **7**, **8**, and **2**), which have a diene with a smaller bite angle, both structures are observed. Duroquinone (**5**) is a special case where the structure is

(8) Dependence of the coordination mode of the Tp^R ligands upon the nature of the other supporting ligand has been observed frequently, as pointed out by a reviewer. For example, replacement of one of the two CO ligands in (κ^3 -Tp^{Me})Rh(CO)₂ by an olefin ligand caused the hapticity change, giving (κ^2 -Tp^{Me})Rh(CO)(olefin).⁶ⁿ

(9) Akita, M.; Takahashi, Y.; Ohta, K.; Miyaji, T.; Moro-oka, Y., unpublished results.

(10) (a) Mn: Kitajima, N.; Singh, U. P.; Amagai, H.; Osawa, M.; Moro-oka, Y. *J. Am. Chem. Soc.* **1991**, *113*, 7757. (b) Fe: Kitajima, N.; Tamura, N.; Tanaka, M.; Moro-oka, Y. *Inorg. Chem.* **1992**, *31*, 3342. (c) Co, Ni: Kitajima, N.; Hikichi, S.; Tanaka, M.; Moro-oka, Y. *J. Am. Chem. Soc.* **1993**, *115*, 5496. (d) Cu: Reference 4.

(11) Ito, M.; Amagai, H.; Fukui, H.; Kitajima, N.; Moro-oka, Y. *Bull. Chem. Soc. Jpn.* **1996**, *69*, 1937.

(12) Rheingold, A. L.; White, C. B.; Trofimenko, S. *Inorg. Chem.* **1993**, *32*, 3471.

(13) Steyn, M. M. de V.; Singleton, E.; Hietkamp, S.; Liles, D. C. *J. Chem. Soc., Dalton Trans.* **1990**, 2991.

(14) Kitajima, N.; Koda, T.; Hashimoto, S.; Kitagawa, T.; Moro-oka, Y. *J. Am. Chem. Soc.* **1991**, *113*, 5664.

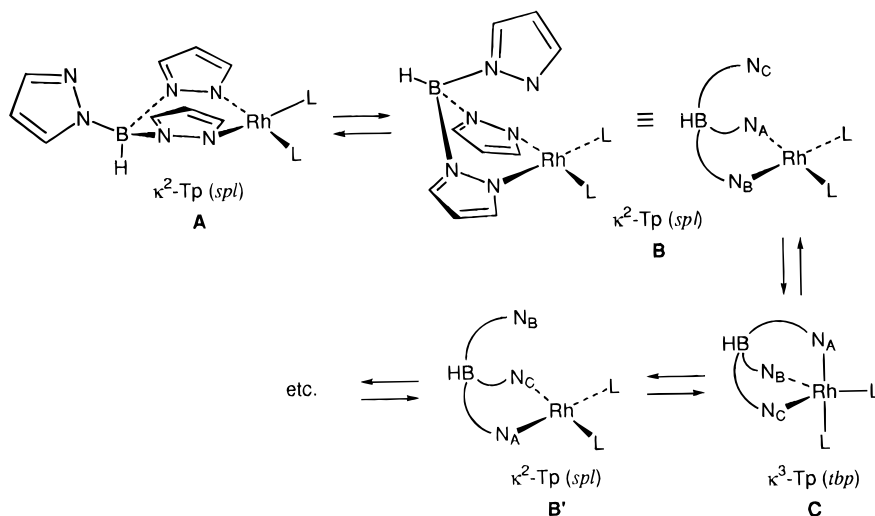
(15) Trofimenko, S.; Calabrese, J. C.; Thompson, J. S. *Inorg. Chem.* **1987**, *26*, 1507.

(16) Gorrell, I. B.; Parkin, J. *Inorg. Chem.* **1990**, *29*, 2452.

(17) Trofimenko, S.; Calabrese, J. C.; Kochi, J. K.; Wolowiec, S.; Hulsbergen, F. B.; Reedijk, J. *Inorg. Chem.* **1992**, *31*, 3943.

(18) Kuchita, M. C.; Dias, H. V. R.; Bott, S. G.; Parkin, G. *Inorg. Chem.* **1996**, *35*, 943.

Scheme 1



dependent on the electronic property of diene. Due to its potential oxidizing ability, its coordination to a Rh center may result in partial oxidation of the metal center to lead to a *tbp* structure, where the Rh center can receive more electrons from the third pyrazolyl ring. On the other hand, no straightforward relationship between the substitution pattern of the pyrazolyl rings and the hapticity of the poly(pyrazolyl)borato ligand has been observed for the nbd complexes (point 2). The κ^2 form is found in **4** (with the nonsubstituted pyrazolyl rings) and **8** (with the 3-Phpz rings), and the κ^3 form is found in **6** and **7** with the pyrazolyl rings methylated at the 3-position, whereas both structures are observed for the 3,5-disubstituted derivative (**2**). Due to this complicated situation, it has been concluded in previous studies that subtle differences in electronic as well as steric environments, including the packing force in crystals, determine the hapticity of the Tp^{R} ligand in the solid state.^{2b,5} We also agree with this statement, and the observation of the two isomeric structures in **2** which cannot be differentiated by ^1H and ^{13}C NMR indicates that the energy barrier for the interconversion is quite low. In addition, it is notable that complex **2** is the first example of a $\text{Tp}^{\text{R}}\text{Rh}(\text{diene})$ -type complex which contains, in a single crystal, two crystallographically independent molecules with κ^2 - and κ^3 - Tp^{R} ligands, and this special situation can give us a clue to discrimination of the two structures on the basis of the IR data, as will be discussed below.

The structural isomerization of $\text{Tp}^{\text{R}}\text{RhL}_2$ -type complexes in solution, as typically indicated by the time-averaged NMR spectra of **1** and **2**, was studied in detail by Venanzi and his co-workers by using IR and various NMR techniques.^{5d} The dynamic behavior has been analyzed as interconversion of the three structural isomers as summarized in Scheme 1: the *spl* structure with a κ^2 - Tp^{R} ligand, where the BH part is located closer to the Rh center than is the noncoordinating pz-N atom (structure **A**),^{5f,6j} the inverted *spl* structure with a κ^2 - Tp^{R} ligand, where the noncoordinating pz-N atom is located closer to the Rh center than is the BH part (structure **B**), and the *tbp* structure with a κ^3 - Tp^{R} ligand (structure **C**). The averaging of the three pyrazolyl rings has been explained by taking into account dissociation of N_B in **C**, which is coordinated to Rh in the original form **B**, leading to another **B**-type structure

(**B'**).^{6j} When this type of process is repeated at a rate faster than the NMR time scale, all the pyrazolyl rings become equivalent. As for diene complexes including **6** and **7**, it is concluded that, in solution, (1) most of the cod complexes exist as the *spl* structure (**B**) with the only exception being the unsubstituted derivative $\text{TpRh}(\text{cod})$, while nbd complexes have more chances to adopt a *tbp* structure as observed for the $\text{HB}(3\text{-i-Pr-4-Br-pz})_3$, $\text{HB}(3\text{-Me-pz})_3$, and $\text{HB}(3,5\text{-Me}_2\text{-pz})_3$ derivatives,^{6d} and (2) interconversion between **B** and **C** occurs much faster than that between **A** and **B** and, therefore, two species, **A** and averaged **B/C**, may be able to be detected by NMR at low temperature. In principle, the coordination structure can be discriminated on the basis of the multinuclear NMR data. However, the dynamic processes occurring faster than the NMR time scale frequently obscure the determination of the coordination structure in solution.

Most of the above features are also observed for the Tp^{iPr} complexes **1** and **2**. One of the features characteristic of the present system is that we could not find any evidence for structure **A**. This is probably due to steric repulsion of the 5-isopropyl substituents, which hinder flipping of the Tp^{iPr} ligand (**B** \rightarrow **A**). Another peculiar spectroscopic feature is that, in the solid state, the nbd complex **2** contains two $\nu(\text{B-H})$ absorptions at 2472 cm^{-1} (**I**) and 2579 cm^{-1} (**II**) (KBr), in contrast to the case for **1**, which has a single absorption at 2475 cm^{-1} (**I**). Comparison of the IR data (Figure 1) and the solid-state structure (Figures 3 and 4) leads to the assignment of the bands **I** and **II** to the B-H stretching vibrations of the *spl* and *tbp* structures, respectively. In other words, bands **I** and **II** can be correlated to the κ^2 - and κ^3 -coordinated Tp^{iPr} ligands, respectively. As for the structure in solution, NMR does not provide any information concerning the coordination geometry because of the fast dynamic process mentioned above. However, IR spectra of **2** recorded in various solvents also contain the two absorptions **I** and **II**, which have the same intensities, and their wavenumbers are essentially the same as those observed as KBr pellets (Table 1). Therefore, the two bands can also be assigned to the *spl* and *tbp* structures with the κ^2 - and κ^3 - Tp^{iPr} ligands, respectively, and any notable change in the **I/II** ratio (ca. 1:1) is observed in the solvents examined. In addition, because (1) in the single crystals, the two

Table 3. Hapticity and $\nu(\text{B-H})$ Values of the Tp^{iPr} Ligand in the Series of $\text{Tp}^{\text{iPr}}\text{ML}_n$ -Type Complexes

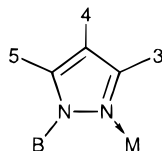
entry no.	complex	coordination geometry ^a	hapticity of Tp^{iPr}	$\nu(\text{B-H})$ (cm^{-1}) ^b	ref
1	$\text{Tp}^{\text{iPr}}\text{Ru}(\text{H})(\text{cod})$	spy	2	2471	9
2	$\text{Tp}^{\text{iPr}}\text{Rh}(\text{mbd})$ (2) ^c	spl	2	2472	this work
3	$\text{Tp}^{\text{iPr}}\text{Rh}(\text{cod})$ (1)	spl	2	2475	this work
4	$\text{Tp}^{\text{iPr}}\text{Pd}(\text{OOBu}^t)\text{py}$	spl	2	2476	9
5	$\text{Tp}^{\text{iPr},t\text{Bu}}\text{Rh}(\text{coe})(\text{CO})$ ^d	spl	2	2486	9
6	$\text{Tp}^{\text{iPr}}\text{M}(\mu\text{-OH})_2\text{MTp}^{\text{iPr}}$ (M = Mn, Fe, Co, Ni, Cu)	spy	3	2527–2543	10
7	$\text{Tp}^{\text{iPr}}\text{Fe}(\text{OC}_6\text{H}_4\text{Me-}p)_2$	tbp	3	2538	11
8	$\text{Tp}^{\text{iPr}}\text{Rh}(\text{mbd})$ (2) ^e	tbp	3	2539	this work
9	$\text{Tp}^{\text{iPr}}\text{Cu}(\mu\text{-O}_2)\text{CuTp}^{\text{iPr}}$	spy	3	2539	4
10	$\text{Tp}^{\text{iPr}}\text{Fe-OC}_6\text{F}_5$	t	3	2540	11
11	$\text{Tp}^{\text{iPr}}\text{Rh}(\text{coe})(\text{NCMe})$	tbp	3	2544	9
12	$\text{Tp}^{\text{iPr}}\text{FeCl}$	t	3	2550	11
13	$\text{Tp}^{\text{iPr}}\text{RhI}_2(\text{NCMe})$	tbp	3	2554	9

^a spl, square planar; tbp, trigonal bipyramidal; spy, square pyramidal; t, tetrahedral. ^b Observed as KBr pellets. ^c Molecule 1. ^d $\text{Tp}^{\text{iPr},t\text{Bu}} = \text{HB}(3\text{-}t\text{-Bu-5-}i\text{-Pr-pz})_3$. ^e Molecule 2.

Table 4. Hapticity and $\nu(\text{B-H})$ Values of the Tp^{R} Ligand in $\text{Tp}^{\text{R}}\text{ML}_n$ -Type Complexes

entry no.	complex	substituents of the pz rings ^a			geometry ^b	hapticity of Tp^{R}	$\nu(\text{B-H})$ (cm^{-1})	ref
		3	4	5				
1	$\text{Tp}^{\text{R}}\text{ZnI}$	mesityl	H	H	t	3	2471	12
2	$[\text{Tp}^{\text{R}}\text{Ru}(\text{CO})_2]_2$	H	H	H	o	3	2485	13
3	$\text{Tp}^{\text{R}}\text{Cu}(\mu\text{-OH})_2\text{CuTp}^{\text{R}}$	Me	H	Me	spy	3	2506	14
4	$[\text{Tp}^{\text{R}}\text{Ni}(\text{NCS})_2]$	Pr^i	Br	H	spy	3	2510	15
5	$\text{Tp}^{\text{R}}\text{Co}(\text{NCS})(\text{THF})$	Ph	H	H	tbp	3	2515	15
6	$\text{Tp}^{\text{R}}\text{Ru}(\text{OCOH})(\text{py})_2$	Me	H	Me	o	3	2519	9
7	$\text{Tp}^{\text{R}}\text{FeCl}$	Bu^t	H	H	t	3	2523	16
8	$\text{Tp}^{\text{R}}\text{Rh}(\text{Cl})(\text{C}_5\text{H}_{11})(\text{CNCH}_2\text{Bu}^t)$	Me	H	Me	o	3	2528	6h
9	$\text{Tp}^{\text{R}}\text{Co}(\text{NCS})$	Bu^t	H	H	t	3	2534	15
10	$\text{Tp}^{\text{R}}\text{Ni}(\text{NCS})$	Bu^t	H	Me	t	3	2542	17
11	$\text{Tp}^{\text{R}}\text{In}$	Bu^t	H	Bu^t	trig	3	2552	18

^a Numbering scheme for the pyrazolyl ring is as shown



^b Abbreviations: spl: square planar; tbp: trigonal bipyramidal; spy, square pyramidal; o, octahedral; t, tetrahedral; trig, trigonal.

structures exist exactly in a 1:1 ratio (Figures 3 and 4) and (2) the intensities of the two bands (KBr) are the same within experimental error, the intensity ratio should roughly correspond to the populations of the *spl* and *tbp* species present in the sample and this argument may be extended to the solution samples. Consequently, almost equal amounts of the two structures *spl* and *tbp* are present in either the solid or solution state and the ratio is not affected significantly by the measurement media.

Thus, the hapticity of the Tp^{iPr} ligand in $\text{Tp}^{\text{iPr}}\text{Rh}$ -(diene) can be deduced from the position of the $\nu(\text{B-H})$ band, i.e. bands around 2470 and 2540 cm^{-1} indicate the presence of a Tp^{iPr} ligand having bidentate (κ^2) and tridentate (κ^3) coordination, respectively.

Dependence of $\nu(\text{B-H})$ Values on Hapticity of the Tp Ligand. In order to examine the generality of the above-mentioned rule, the $\nu(\text{B-H})$ values, hapticities of the Tp^{R} ligands, and coordination structures of various structurally characterized $\text{Tp}^{\text{R}}\text{ML}_n$ -type complexes are compared as listed in Tables 3 and 4.

In Table 3, $\text{Tp}^{\text{iPr}}\text{ML}_n$ -type complexes (entries 1–4 and 6–13) and a *t*-Bu derivative (entry 5) synthesized in our laboratory are summarized according to the increasing order of the $\nu(\text{B-H})$ values. The rule holds true irrespective of the central metal (the first- and second-row transition metals), the coordination geometry, and the other ligands (L). The ($\kappa^3\text{-Tp}^{\text{iPr}}$) ML_n -type complexes

show the $\nu(\text{B-H})$ band in the range of 2527–2554 cm^{-1} , whereas the $\nu(\text{B-H})$ band of the ($\kappa^2\text{-Tp}^{\text{iPr}}$) ML_n -type complexes is observed in the narrow range of 2471–2486 cm^{-1} (italicized in Table 3). The Rh and Pd complexes (entries 2–5) are 16e square-planar d^8 complexes, and the square-pyramidal Ru complex $\text{Tp}^{\text{iPr}}\text{Ru}(\text{H})(\text{cod})$ (entry 1) is isoelectronic with **1**. No $\nu(\text{B-H})$ vibration has been observed in the range 2486–2527 cm^{-1} for $\text{Tp}^{\text{iPr}}\text{ML}_n$ -type complexes, and therefore, the $\nu(\text{B-H})$ values turn out to be diagnostic of the two coordination modes of the Tp^{iPr} ligand ($\kappa^2 < 2500 \text{ cm}^{-1} < \kappa^3$).

Data for structurally characterized $\text{Tp}^{\text{R}}\text{ML}_n$ derivatives bearing other substituted Tp^{R} ligands are listed in Table 4. All the examples contain a tridentate Tp^{R} ligand (κ^3). Although several ($\kappa^2\text{-Tp}^{\text{R}}$) ML_n -type complexes have been characterized crystallographically, their $\nu(\text{B-H})$ values were not reported in the original papers and therefore systematic comparisons taking into account the $\nu(\text{B-H})$ vibrations cannot be discussed in detail. The $\nu(\text{B-H})$ values for ($\kappa^3\text{-Tp}^{\text{R}}$) ML_n -type complexes vary in the range 2476–2552 cm^{-1} , overlapping the signals for ($\kappa^2\text{-Tp}^{\text{iPr}}$) ML_n (Table 3). This should come from the effect of the substituents attached to the pyrazolyl rings. In general, as the substituents become more electron-donating, the B–H stretching vibrations shift to higher energy.¹⁹ For example, replacement of the methyl substituents in the dicopper μ -hydroxo

complex $\text{Tp}^{\text{Me}}\text{Cu}(\mu\text{-OH})_2\text{CuTp}^{\text{Me}}$ ($\nu(\text{B-H})$ 2506 cm^{-1}) (entry 3, Table 4), with the isopropyl groups results in a 21 cm^{-1} shift to higher energy ($\text{Tp}^{\text{iPr}}\text{Cu}(\mu\text{-OH})_2\text{CuTp}^{\text{iPr}}$; $\nu(\text{B-H})$ 2527 cm^{-1} ; entry 6, Table 3). Thus, the value 2500 cm^{-1} is not valid as a general turning point for discrimination of the two coordination modes of the Tp^{R} ligands bearing substituents other than the isopropyl groups. However, if we take into account the substituent effect discussed above, the coordination mode may be discriminated on the basis of the $\nu(\text{B-H})$ values in a manner similar to that for the $\text{Tp}^{\text{iPr}}\text{ML}_n$ complexes, and the $\nu(\text{B-H})$ band for a bidentate complex, $(\kappa^2\text{-Tp}^{\text{R}})\text{ML}_n$, is anticipated to appear in the lower energy region compared to that for a tridentate complex, $(\kappa^3\text{-Tp}^{\text{R}})\text{ML}_n$.

Conclusion

The two rhodium–diene complexes $\text{Tp}^{\text{iPr}}\text{Rh}(\text{cod})$ (**1**) and $\text{Tp}^{\text{iPr}}\text{Rh}(\text{nbd})$ (**2**) have been synthesized and characterized spectroscopically and crystallographically. On the basis of (**1**) the two $\nu(\text{B-H})$ bands observed for the two different structures (*spi* and *tbp*) of **2** and (2) comparison with **1**, it is established that the $\nu(\text{B-H})$ value is a good indicator for the hapticity of the Tp^{iPr} ligand. The hapticity change of Tp^{R} ligands has been a subject of previous studies (in particular, for $\text{Tp}^{\text{R}}\text{RhL}_2$ complexes), which employ mainly NMR and crystallography for analysis of the structure and the dynamic processes. The present study clearly points out that the $\nu(\text{B-H})$ band can be used as a convenient criterion complementary to the NMR and X-ray analysis.

Because Tp^{R} ligands have been employed usually to synthesize complexes with a tripodal $\kappa^3\text{-Tp}^{\text{R}}$ ligand, examples of $(\kappa^2\text{-Tp}^{\text{R}})\text{ML}_n$ complexes are rare except for the 16e square-planar d^8 complexes and, therefore, little attention has been paid to such types of complexes. A bidentate species, $(\kappa^2\text{-Tp}^{\text{R}})\text{ML}_n$, can be formed via dissociation of one of the three pyrazole rings in $(\kappa^3\text{-Tp}^{\text{R}})\text{ML}_n$, as detailed in Scheme 1, and the resulting coordinatively unsaturated species may work as a reactive intermediate, which may be readily detected by IR measurements as established by the present study.

Experimental Section

General Methods. All manipulations were carried out under an inert atmosphere by using standard Schlenk tube techniques. Ether (Na–K alloy), CH_2Cl_2 (P_2O_5), and MeOH ($\text{Mg}(\text{OMe})_2$) were treated with appropriate drying agents, distilled, and stored under argon. KTp^{iPr} and $[\text{RhCl}(\text{diene})]_2^{20}$ were prepared according to the published procedures. Other chemicals were purchased and used as received. ^1H and ^{13}C NMR spectra were recorded on Bruker AC200 (^1H , 200 MHz) and JEOL GX-270 (^1H , 270 MHz; ^{13}C , 67 MHz) spectrometers. Solvents for NMR measurements containing 0.5% TMS were dried over molecular sieves, degassed, distilled under reduced

(19) The electron-donating ability of the Tp^{R} ligands may be evaluated on the basis of the $\nu(\text{B-H})$ value of NaTp^{R} and KTp^{R} , as pointed out by one of the reviewers, although few of them have been characterized crystallographically. K salts: $[\text{K}[\text{HB}(3,5\text{-Bu}_2\text{pz})_3]]$, 2549 cm^{-1} ; $[\text{K}[\text{HB}(3\text{-Bu}^t\text{-5-Pr-pz})_3]]$, 2468 cm^{-1} ; KTp^{iPr} , 2464 cm^{-1} ; KTp^{Me} , 2438 cm^{-1} . Na salts: $[\text{Na}[\text{HB}(3,5\text{-Pr}^t\text{-4-Br-pz})_3]]$, 2486 cm^{-1} ; NaTp^{iPr} , 2478 cm^{-1} ; $[\text{HB}(3,5\text{-Me}_2\text{-4-Brpz})_3]$, 2479 cm^{-1} ; NaTp^{Me} , 2452 cm^{-1} (KBr pellets). However, the relationship is not straightforward, because, for example, introduction of the electron-withdrawing Br atom at the 4-position causes a higher energy shift.

(20) (a) cod complex: Giordano, G.; Crabtree, R. H. *Inorg. Synth.* **1979**, *19*, 218. (b) nbd complex: Abel, E. W.; Bennett, M. A.; Wilkinson, G. *J. Chem. Soc.* **1959**, 3178.

Table 5. Crystallographic Data for **1** and **2**

	1	2
formula	$\text{C}_{35}\text{H}_{58}\text{BN}_6\text{Rh}$	$\text{C}_{34.5}\text{H}_{56}\text{BNO}_{0.5}\text{Rh}$ ($2 \cdot 1/2\text{MeOH}$)
fw	676.6	676.6
cryst syst	triclinic	monoclinic
space group	$P\bar{1}$	$P2_1/c$
<i>a</i> (Å)	10.870(2)	16.298(4)
<i>b</i> (Å)	17.641(4)	13.560(4)
<i>c</i> (Å)	10.144(2)	33.36(1)
α (deg)	102.48(1)	
β (deg)	95.00(1)	97.39(3)
γ (deg)	78.76(1)	
<i>V</i> (Å ³)	1860.6(6)	7312(4)
<i>Z</i>	2	8
d_{calcd} (g cm^{-3})	1.21	1.23
μ (cm^{-1})	4.88	4.98
temp (°C)	25	25
2 θ (deg)	5–50	5–50
no. of data collected	6912	13 956
no. of data with $I > 3\sigma(I)$	5301	8543
no. of variables	388	775
<i>R</i>	0.042	0.045
<i>R_w</i>	0.038	0.037

pressure, and stored under Ar. IR spectra were obtained on a JASCO FT/IR 5300 spectrometer.

Synthesis of $\text{Tp}^{\text{iPr}}\text{Rh}(\text{cod})$ (1**).** To $[\text{RhCl}(\text{cod})]_2$ (208 mg, 0.422 mmol) dissolved in CH_2Cl_2 (8 mL) was added KTp^{iPr} (427 mg, 0.846 mmol). After the mixture was stirred for 10 min at ambient temperature, the volatiles were removed under reduced pressure and the residue was extracted with hexanes (20 mL). Salts were removed by filtration through a Celite plug, and the solvent was removed again under reduced pressure. Crystallization of the residue from ether–MeOH at -20 °C gave **1** as orange prisms (327 mg, 0.483 mmol, 58% yield). δ_{H} (CDCl_3): 6.03 (3H, s, pz), 4.38 (2H, br s, olefinic protons of cod), 3.35–3.27 (6H, m, CH), 2.14–2.11 (4H, m, CH_2 in cod), 1.56 (2H, br s, CH_2 in cod), 1.52 (2H, br s, CH_2 in cod), 1.35 (18H, d, $J = 6.9$ Hz, CH_3), 1.24 (18H, d, $J = 6.9$ Hz, CH_3). δ_{C} (CDCl_3): 159.3 (s, pz), 156.7 (s, pz), 98.3 (d, $J = 170$ Hz, pz), 79.4 (dd, $J_{\text{C-H}} = 163$ Hz and $J_{\text{C-Rh}} = 12$ Hz, olefinic carbon atoms of cod), 29.7 (t, $J = 127$ Hz, cod), 28.1 (d, $J = 128$ Hz, CH), 26.3 (d, $J = 128$ Hz, CH), 23.6 (q, $J = 126$ Hz, CH_3), 23.3 (q, $J = 126$ Hz, CH_3). Anal. Calcd for $\text{C}_{35}\text{H}_{58}\text{BN}_6\text{Rh}$: C, 62.13; H, 8.64; N, 12.42. Found: C, 61.60; H, 8.65; N, 12.48.

Synthesis of TiTp^{iPr} . To a CH_2Cl_2 solution (20 mL) of KTp^{iPr} (1.50 g, 2.97 mmol) was added TIOAc (1.01 g, 3.23 mmol). After the mixture was stirred overnight, the resulting salts were removed by filtration through a Celite pad. The volatiles were removed under reduced pressure, and the product was isolated as a white solid by crystallization from ether–MeOH. TiTp^{iPr} (1.21 g, 1.80 mmol, 61% yield): δ_{H} (C_6D_6) 5.96 (3H, s, pz), 3.69 (3H, sept, $J = 6.8$ Hz, CH), 3.30–3.05 (3H, m, CH), 1.23 (18H, d, $J = 6.8$ Hz, CH_3), 1.21 (18H, d, $J = 6.8$ Hz, CH_3). IR (KBr) 2539 cm^{-1} . Anal. Calcd for $\text{C}_{27}\text{H}_{46}\text{BN}_6\text{Ti}$: C, 48.41; H, 6.92; N, 12.55. Found: C, 48.27; H, 6.85; N, 12.60.

Synthesis of $\text{Tp}^{\text{iPr}}\text{Rh}(\text{nbd})$ (2**).** To a CH_2Cl_2 solution (5 mL) of $[\text{RhCl}(\text{nbd})]_2$ (156 mg, 0.339 mmol) was added a CH_2Cl_2 solution (5 mL) of TiTp^{iPr} (228 g, 0.346 mmol) dropwise. After the mixture was stirred at ambient temperature, the resulting insoluble materials were removed by filtration through a Celite pad. Removal of the volatiles under reduced pressure followed by crystallization from ether–MeOH gave **2** as brown prisms (203 mg, 0.307 mmol, 88% yield). δ_{H} (CDCl_3): 5.81 (3H, s, pz), 3.56 (4H, s, olefinic protons of nbd), 3.35 (3H, sept, $J = 6.9$ Hz, CH), 3.20 (3H, sept, $J = 6.9$ Hz, CH), 1.27 (18H, d, $J = 6.9$ Hz, CH_3), 1.13 (18H, d, $J = 6.9$ Hz, CH_3), 1.27–1.13 (4H, m, remaining nbd protons overlapped with the CH_3 signal). δ_{C} (CDCl_3): 160.6 (s, pz), 155.5 (s, pz), 97.6 (d, $J = 170$ Hz, pz), 59.4 (d, $J = 131$ Hz, CH_2 carbon atom of nbd), 48.8 (d, $J = 150$ Hz, bridgehead carbon atom of nbd), 42.8 (dd, $J_{\text{C-H}} = 176$ Hz and $J_{\text{C-Rh}} = 10$ Hz, olefinic

carbon atoms of nbd), 27.4 (d, $J = 128$ Hz, CH), 26.2 (d, $J = 128$ Hz, CH), 24.0 (q, $J = 126$ Hz, CH₃), 23.5 (q, $J = 126$ Hz, CH₃). Anal. Calcd for C₃₄H₅₄BN₆Rh: C, 61.82; H, 8.24; N, 12.72. Found: C, 61.34; H, 8.25; N, 12.97.

Experimental Procedure for X-ray Crystallography.

Suitable single crystals were mounted on glass fibers, and diffraction measurements were made on a Rigaku AFC-5R automated four-circle diffractometer by using graphite-monochromated Mo K α radiation ($\lambda = 0.710\ 59$ Å). The unit cells were determined and refined by a least-squares method using 20 independent reflections ($2\theta \approx 20^\circ$). Data were collected with $2\theta-\omega$ (**1**) and ω scan techniques (**2**). If $\sigma(F)/F$ was more than 0.1, a scan was repeated up to three times and the results were added to the first scan. Three standard reflections were monitored every 150 measurements. The data processing was performed on a Micro Vax II computer (data collection) and an IRIS Indigo computer (structure analysis) by using the teXsan structure solving program system obtained from the Rigaku Corp., Tokyo, Japan. Neutral scattering factors were obtained from the standard source.²¹ In the reduction of data, Lorentz and polarization corrections and an empirical absorp-

tion correction (Ψ scan) were made. Crystallographic data and the results of refinements are summarized in Table 5.

The structures were solved by a combination of direct methods and Fourier synthesis (SAPI91 and DIRDIF). All the non-hydrogen atoms were refined anisotropically, and all the hydrogen atoms were located at the calculated positions and were not refined.

Acknowledgment. We are grateful to the Ministry of Education, Science, Sports and Culture of the Japanese Government for financial support of the research.

Supporting Information Available: Tables of positional parameters and B_{eq} values, anisotropic thermal parameters, and bond lengths and angles for **1** and **2** (11 pages). Ordering information is given on any current masthead page.

OM970352N

(21) *International Tables for X-Ray Crystallography*, Kynoch Press: Birmingham, U.K., 1975; Vol. 4.